Chinese Chemical Letters 37 (2026) 111940

Contents lists available at ScienceDirect

Chinese Chemical Letters

journal homepage: www.elsevier.com/locate/cclet

Synthesis of antifungal gem–difluoroallylsilane compounds via radical transfer strategy

Fuyang Yue[1], Fei Yuan[1], Kun Li[1], Xun Luo, Hongjian Song, Yuxiu Liu, Qingmin Wang*

State Key Laboratory of Elemento-Organic Chemistry, Research Institute of Elemento-Organic Chemistry, Frontiers Science Center for New Organic Matter, College of Chemistry, Nankai University, Tianjin 300071, China

ARTICLE INFO

Article history:
Received 21 June 2025
Revised 24 September 2025
Accepted 9 October 2025
Available online 10 October 2025

Keywords:
Antifunga
Photoredox
Difluoroallylsilane
Radicals
Trifluoroolefins

ABSTRACT

gem–Difluorovinyl compounds and silicon-containing compounds are valuable structural units in organic and medicinal chemistry. However, they are mostly found separately in most compounds. In this study, we present a photocatalytic approach for the synthesis of *gem*–difluorovinylsilanes, using readily accessible silylboronic pinacol esters as reagents. Through a radical transfer strategy, this method overcomes the limitation of their high oxidation potential. Biological assays further confirmed that several target compounds exhibited moderate to potent antifungal activity against plant pathogens, including *Botrytis cinerea*, *Setosphaeria turcica* and *Rhizoctonia solani*.

© 2026 Published by Elsevier B.V. on behalf of Chinese Chemical Society and Institute of Materia Medica, Chinese Academy of Medical Sciences.

Silicon, belonging to Group IV elements, ranks as the second most abundant element in both the Earth's crust surface and soils [1–3]. Silicone–based organosilicon compounds possess distinct advantages such as controllable sol–gel condensation, lipophilicity, and low surface tension owing to their unique structure [4–6]. As a result, silicone compounds, serving as crucial raw materials, have assumed an indispensable role in materials science, polymer chemistry, and agrochemistry (Fig. 1A) [7–12]. With the development of organic photo/electrocatalysis, chemoselective silylation *via* silyl radicals holds great potential in the industrial realm (Fig. 1B, left) [13,14]. Typically, silyl radicals are generated through the direct activation of Si–H bonds [15–23]. Silylboronic pinacol esters, containing Si–B bonds, possess advantages such as good stability, commercial availability, and ease of preparation [24,25], and they have the potential to generate silane radicals. Nevertheless, silylboronic pinacol esters have a high oxidation potential (approximately +2.0 V *vs.* SCE). This high oxidation potential makes it more challenging to cleave the Si–B bond under photoredox conditions [26]. The conventional method of activating Si–B bonds usually involve introducing nucleophilic reagents to coordinate with boron in order to lower the redox potential (Fig. 1B, right) [26]. Amine radicals, frequently used as radical transfer reagents in photocatalysis, have been demonstrated to drive C–B bond activation to generate carbon-radicals [27–32]. We believe that they also hold excellent synthetic potential for use in the activation of silylboronic pinacol esters.

Fluorine–containing compounds endow drug molecules with advantages such as enhanced lipophilicity, specific conformation, and improved bioavailability [33–40]. In recent years, with the continuous maturation of synthetic techniques, the number of fluorine–containing drugs and pesticides featuring complex structures has been on the rise [40]. *gem*–Difluorovinyl compounds have attracted extensive interest from researchers due to their isosteric relationship with carbonyl groups [41–48].

Given the unique properties of silicon–containing organic compounds, we postulate that introducing both "Si" atoms and *gem*–difluoroalkene fragments into the same molecule may offer medicinal chemists a novel perspective. Inspired by the research advancements, we devise a radical transfer strategy for generating silane radicals. Under visible–light irradiation, the catalyst transforms the amine into amine radicals, which in turn induce the cleavage of the Si–B bond to generate silyl radicals. This approach successfully enables the defluorination of trifluoroolefins for the synthesis of fluorine–containing organosilicon compounds under mild reaction conditions (Fig. 1C). This study synthesized novel difluoromethylsilane compounds, showing potent fungicidal activity (inhibition rates >60%) against major plant pathogens at 50 μg/mL. Their EC_{50} values compared favorably with commercial fungicides. DFT and MEP analyses linked activity to molecular orbital distributions and electrostatic properties.

In our initial experiments, we selected 1-(benzyloxy)-4-(3,3,3-trifluoroprop-1-en-2-yl)benzene (**1a**) and triethyl(4,4,5,5-

* Corresponding author.
E-mail address: wangqm@nankai.edu.cn (Q. Wang).
[1] These authors contributed equally to this work.

https://doi.org/10.1016/j.cclet.2025.111940
1001-8417/© 2026 Published by Elsevier B.V. on behalf of Chinese Chemical Society and Institute of Materia Medica, Chinese Academy of Medical Sciences.

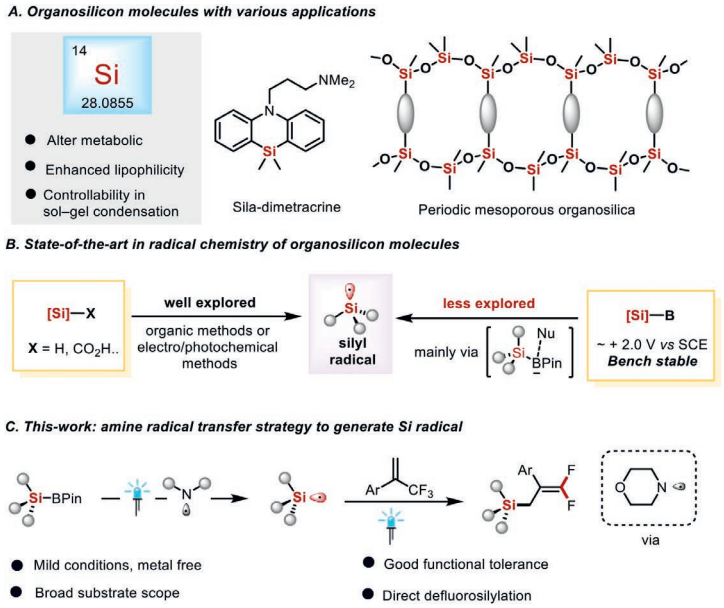
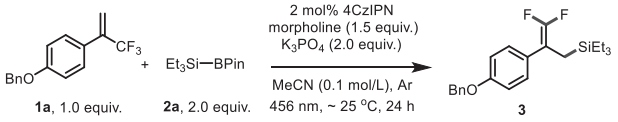


Fig. 1. From inspiration to reaction design. (A) Organosilicon molecules with various applications. (B) State-of-the-art in radical chemistry of organosilicon molecules. (C) This-work: amine radical transfer strategy to generate Si radical.

Table 1
Optimization of conditions for addition reaction between 1-(benzyloxy)-4-(3,3,3-trifluoroprop-1-en-2-yl)benzene (**1a**) with triethyl(4,4,5,5-tetramethyl-1,3,2-dioxaborolan-2-yl)silane **2a**.[a]



1a, 1.0 equiv. **2a**, 2.0 equiv. **3**

Entry	Deviation from standard conditions	Yield (%)[b]
1	None	85 (83[c])
2	$Ir[dF(CF_3)ppy]_2(dtbbpy)PF_6$ as PC	77
3	Piperidine as activation reagent	30
4	*n*-Butylamine as activation reagent	NR
5	Dichloromethane as solvent	70
6	Toluene as solvent	NR
7	Na_2CO_3 as base	65
8	Cs_2CO_3 as base	82
9	No morpholine	NR
10	No PC/light	NR
11	Under air	30

[a] Standard conditions: **1a** (0.2 mmol), **2a** (0.4 mmol), photocatalyst (PC, 0.004 mmol), morpholine (0.3 mmol), K_3PO_4 (0.4 mmol), MeCN (2 mL), Ar, 456 nm LED, r.t., 24 h.
[b] Yields were determined by ^{19}F NMR spectroscopy with fluorobenzene as an internal standard. NR = no reaction.
[c] Isolated yield.

tetramethyl-1,3,2-dioxaborolan-2-yl)silane (**2a**) as model substrates (Table 1). A solution of these substrates in dry acetonitrile ([**1a**] = 0.1 mol/L) was prepared, containing 4CzIPN (2 mol%) as a photocatalyst, morpholine (1.5 equiv.) as an activation reagent, and K_3PO_4 (2 equiv.) as a base. This solution was irradiated with a 456 nm LED at room temperature (~25 °C) under an argon atmosphere for 24 h. As a result, the desired addition product **3** was obtained in an 85% yield (entry 1).

We tested various other photocatalysts, such as $Ir[dF(CF_3)ppy]_2(dtbbpy)PF_6$ (entry 2; for more detailed information, please refer to Supporting information for details). However, 4CzIPN was found to be the optimal choice. Different activation reagents were also evaluated. Piperidine and *n*–butylamine led to lower yields of product **3** (31% and trace amounts, respectively; entries 3 and 4). Solvent screening indicated that dichloromethane gave slightly lower yields of **3** compared to acetonitrile (compare entry 1 with entry 5), while toluene gave a relatively low yield, with only trace amounts detected. The other solvents tested yielded <45% (see Supporting information for details). When we replaced K_3PO_4 with Na_2CO_3 or Cs_2CO_3 as the base, the yields of **3** decreased to 65% and 82%, respectively (entries 7 and 8). Control experiments confirmed that the activation reagent, the photocatalyst, light, and the exclusion of oxygen were all essential for this transformation (entries 9–11).

After identifying the optimized conditions, we explored the substrate scope for the synthesis of fluorinated organosilicon compounds through the defluorination functional-group reaction between α-trifluoromethyl arylalkene and silylboronic pinacol esters derivatives (Fig. 2). These conditions were widely applicable to **1** and demonstrated excellent selectivity and functional-group compatibility. Electron–withdrawing groups attached to the phenyl ring were well–tolerated, resulting in good yields (45%–51%) of the corresponding *gem*–difluoroalkenes **4**–**5**. We observed that when the para-position of the phenyl ring in the arylalkene was substituted with electron–donating groups such as methyl, *n*-propyl, or methoxy, the corresponding products **6**–**14** were produced with yields ranging from moderate to excellent (64%–81%).

However, when the *meta*–position was substituted with an aryl ring or a methoxy group, the yields decreased slightly (**15**–**16**, 61%–62%). By placing bisubstituted groups at different positions on the benzene ring, the desired products **17**–**21** were obtained with moderate yields (52%–68%). Alkenes with trifluoromethyl groups located on the benzene ring were poorly tolerated in this reaction system, yielding the product in only 41% (**22**). When α-trifluoromethyl alkenes containing heterocycles such as dibenzo[*b,d*]thiophene-4-yl and naphthalene-2-yl moieties were used, the corresponding products **23**–**24** were obtained in moderate yields (49%–55%). Next, we explored the reaction scope of silylboronic pinacol esters using compound **1a** as the free–radical acceptor (Fig. 2). As shown, various silylboronic pinacol esters bearing different sterically diverse substituents, including triisopropyl, dimethylethyl, and dimethyl–*tert*–butyl groups, as well as some primary silylboronic pinacol esters, successfully reacted with α-trifluoromethyl arylalkene **1a**. This reaction afforded the

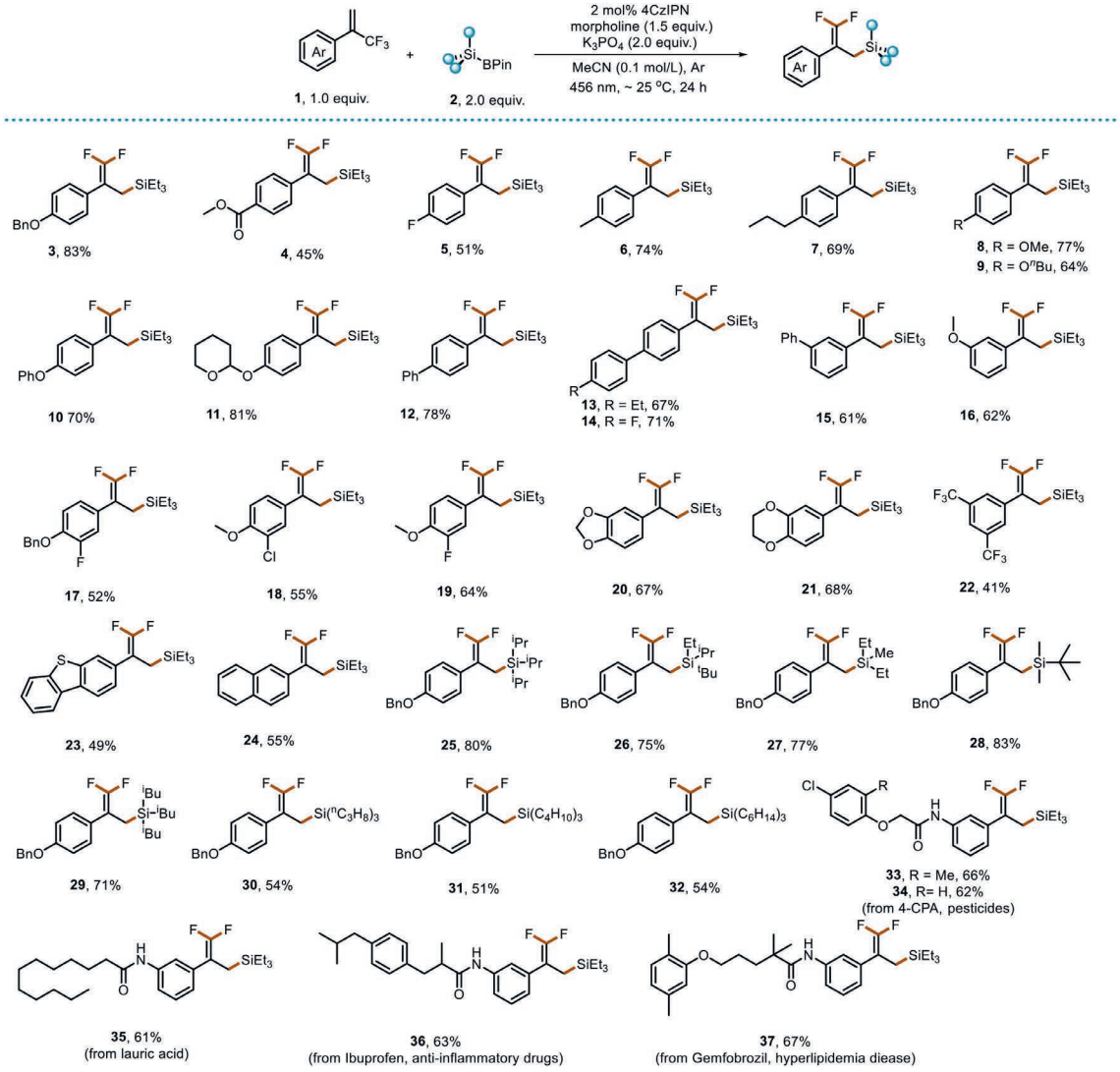


Fig. 2. Substrate scope of the deboronative functionalization reaction. Reaction conditions: **1** (0.2 mmol), **2** (0.4 mmol), photocatalyst (2 mol%), morpholine (0.3 mmol, 1.5 equiv.), 456 nm LED, solvent (2.0 mL, [**1**] = 0.1 mol/L), ~25 °C, Ar, 24 h. Isolated yields are reported.

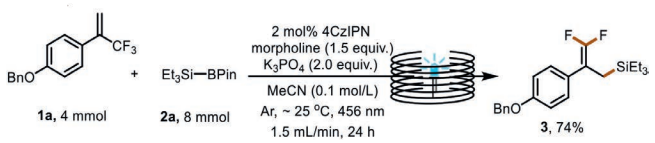


Fig. 3. Gram-scale reaction in continuous-flow.

desired products **25**–**32** in yields ranging from 51 % to 83 %. Subsequently, for further evaluating the applicability of this reaction, various complex α-trifluoromethyl arylalkene-derived from natural products **33**–**37** were subjected to the methodology.

To further demonstrate the synthetic potential of our method, we carried out a gram-scale continuous-flow reaction to synthesize the difluoroketone compound (Fig. 3). With a flow rate of 1.5 mL/min and a residence time of 24 h, we were able to scale up the reaction to 4 mmol.

Plant-pathogenic fungi pose a serious threat to global food security and ecosystems. Chemical control is an effective means of preventing and managing fungal diseases [49,50]. However, the repeated long-term use of fungicides with a single mode of action can lead to resistance issues. An effective approach to developing new fungicides is the construction of new fungicide skeletons through organic synthesis methodology [51–54]. Compounds containing silicone that are environmentally compatible and exhibit synergistic effects have attracted considerable attention in the field of drug discovery and development [1–12]. Using this method, we successfully synthesized a series of novel *gem*–difluoroallylsilane compounds and investigated their fungicidal properties.

The mycelial growth rate method was used to test the fungicidal activity of the *gem*–difluoroallylsilane skeleton compounds against 10 pathogenic fungi at a concentration of 50 μg/mL. Commercial fungicides pyraclostrobin and boscalid were selected as positive controls (Table S6 in Supporting information). Some of the target compounds exhibited potent fungicidal activity against *Botrytis cinerea*, *Setosphaeria turcica* and *Rhizoctonia solani*. Most of these compounds exhibited inhibitory activity against *B. cinerea* of greater than 60 %, with compounds **13–15** inhibiting it by >75 %. Compounds **3**, **8**, **11**, **18** and **19** exhibited an inhibition rate of over 70 % against *S. turcica*, while compounds **13**, **14**, **15**, **23**, **26** and **33** demonstrated an inhibition rate of over 60 % against *R. solani*. Compound **13** exhibited relatively broad-spectrum antifungal activity, with inhibition rates exceeding 60 % against four phytopathogenic fungi. These results suggest that the *gem*–difluoroallylsilane skeleton has fungicidal properties. Compounds with an inhibition rate

Table 2
In vitro EC_{50} values of selected compounds.

Fungi	Compd.	Regression equation	R^2	95 % Confidence interval (μg/mL)	EC_{50} (μg/mL)
Botrytis cinerea	**13**	$y = 4.5427 + 1.2071x$	0.9872	1.88~3.04	2.39
	14	$y = 4.5881 + 0.9622x$	0.9763	1.95~3.68	2.70
	15	$y = 4.5924 + 0.8318x$	0.9931	2.63~3.63	3.09
	Pyraclostrobin	$y = 4.8688 + 1.1423x$	0.9848	1.01~1.68	1.30
	Boscalid	$y = 5.1283 + 0.6203x$	0.9940	0.52~0.74	0.62
Setosphaeria turcica	**3**	$y = 4.3497 + 0.9109x$	0.9941	4.50~5.95	5.17
	8	$y = 4.7167 + 0.6894x$	0.9947	2.22~2.99	2.58
	19	$y = 4.4631 + 0.7848x$	0.9975	4.42~5.28	4.83
	Boscalid	$y = 4.6064 + 0.8838x$	0.9869	2.43~3.62	2.97
	Pyraclostrobin	$y = 4.8242 + 0.7066x$	0.9967	1.57~2.00	1.77
Rhizoctonia solani	**14**	$y = 3.8433 + 0.9925x$	0.9571	10.47~20.45	14.64
	33	$y = 4.0386 + 1.0456x$	0.9926	7.14~9.67	8.31
	Boscalid	$y = 4.7168 + 1.3325x$	0.9745	1.20~2.22	1.63
	Pyraclostrobin	$y = 6.1866 + 0.8004x$	0.9942	0.02~0.04	0.03

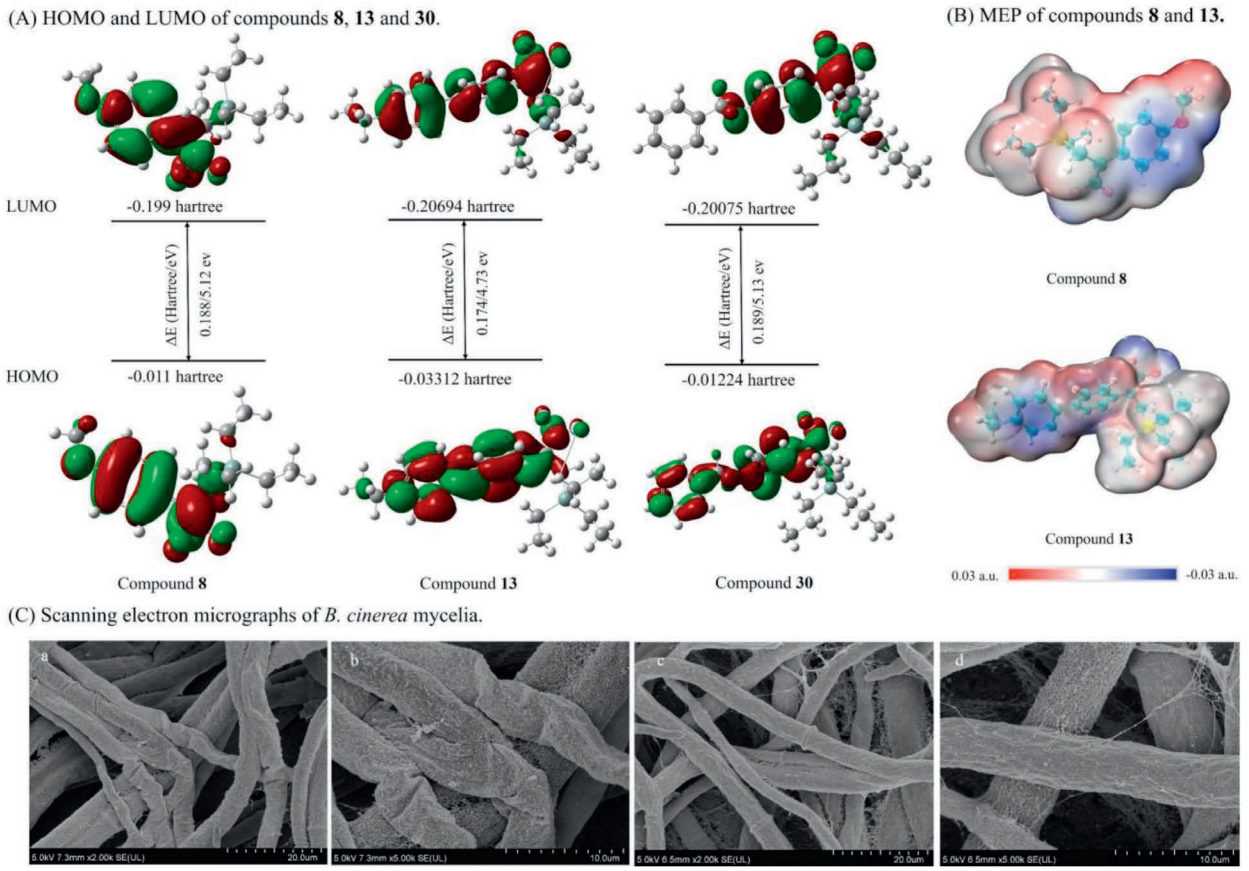


Fig. 4. Frontier molecular orbitals (HOMO and LUMO) and molecular electrostatic potential (MEP) surfaces of target compounds. (A) HOMO and LUMO of compounds **8**, **13** and **30**. (B) MEP of compounds **8** and **13**. (C) Scanning electron micrographs of *B. cinerea* mycelia: (a, b) Compound **13**, treated with 0.5 % DMF plus the compound **13** at 4.78 μg/mL; (c, d) control, treated with 0.5 % DMF.

greater than 75 % were selected for EC_{50} activity determination (Table 2). For *B. cinerea*, the EC_{50} values of compounds **13–15** ranged from 2.39 μg/mL to 3.09 μg/mL, which are lower than those of the commercial fungicides pyraclostrobin (1.30 μg/mL) and pydiflumetofen (0.62 μg/mL). Compound **8** (2.58 μg/mL) exhibited comparable activity to boscalid (2.97 μg/mL) against *S. turcica*, but was less effective than pyraclostrobin (1.77 μg/mL). Compounds **8** and **13** showed good antifungal activity and could serve as lead compounds for further structural optimization and mode-of-action studies. For *R. solani*, the EC_{50} values of compound **14** and **33** were determined to be 14.64 and 8.31 μg/mL, respectively. Although both compound **14** and **33** demonstrated inhibitory effects against *R. solani*, their potency was lower than that of the commercial fungicides boscalid (1.63 μg/mL) and pyraclostrobin (0.03 μg/mL). This class of compounds can serve as lead fungicides for structural optimization and mechanism-of-action studies.

To further investigate the structural properties underlying the antifungal activity of target compounds, density functional theory (DFT) calculations were performed on the high-activity compounds **8** and **13**, as well as the low-activity compound **30**. The electron distributions of the HOMO and LUMO for the highly active compounds **8** and **13** were similar. In contrast, the LUMO of the low-activity compound **30** was mainly distributed over the benzene ring and the *gem*–difluoroalkene moiety. This suggested that varia-

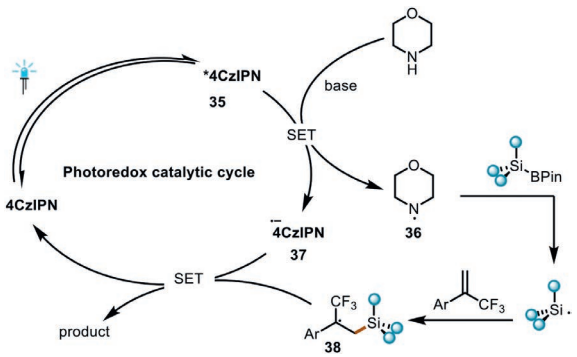


Fig. 5. Proposed mechanism.

tions in substituents on the benzene ring significantly impact biological activity (Fig. 4A). Fig. 4B shows that, for compounds **8** and **13**, the MEP maps indicate that the *gem*–difluoroalkenyl group is located in the negative electrostatic potential region (blue), suggesting nucleophilic characteristics. Meanwhile, the silyl group and aromatic ring are situated in the positive potential region (red), indicating electrophilic properties. Optimizing the electrostatic potential around the active core region (*e.g.*, the aromatic ring) facilitates effective interaction with fungal receptors or enzyme active sites. These results imply that variations in factors such as energy levels, molecular orbital distribution and MEP characteristics may account for differences in antifungal activity by affecting receptor interactions.

Subsequently, the effect of active compound **13** on the mycelial morphology of *B. cinerea* was observed using scanning electron microscopy. The results were shown in Fig. 4C. After treatment with compound **13**, the mycelia exhibited obvious collapse and shrinkage, while the mycelial structure in blank control maintained smooth and regular. This result indicated that compound **13** could disrupt the mycelial morphology, thereby interfering with the normal growth of *B. cinerea*.

To gain insight into the reaction pathway, several control experiments were performed. We conducted a light/dark experiment (see Supporting information for details); the results revealed that in the absence of light, the reaction halted. This suggests that continuous visible-light irradiation is essential for this amination reaction to proceed. A series of cyclic voltammetry measurements were carried out with Ag/AgCl as a reference electrode in CH_3CN using tetrabutylammonium perchlorate as a supporting electrolyte. The purpose was to determine the possible changes in oxidation-reduction potential after adding morpholine. The cyclic voltammetry results showed that the oxidation peak potential of morpholine ($E = +0.95$ V *vs.* SCE) was lower than that of the silylboronic pinacol esters ($E = +1.94$ V *vs.* SCE), indicating that morpholine would be preferentially oxidized (see Supporting information for details). Furthermore, adding morpholine to the silylboronic pinacol esters did not result in a shift in the NMR signal of [^{11}B], suggesting that no direct complex was formed between morpholine and the silylboronic pinacol esters (see Supporting information for details).

On the basis of the above-mentioned experiments and literature reports, we propose the reaction mechanism (Fig. 5): Initially, photocatalyst is excited by light irradiation giving excited state of photocatalyst **35**. morpholine quenches the excited-state photocatalyst to generate an amine radical **36** *via* the SET process and lead to the transformation from **35** to **37**. Then amine radical **36** interacts with the boron species to liberate the corresponding silyl radical. Subsequently, the silyl radical undergoes a Michael addition reaction with the α-trifluoromethyl alkenes to generate the CF_3-styrene carbon radical **38**, Single-electron reduction of the CF_3-styrene carbon radical by **37** generates the CF_3-styrene carbanion intermediate, which undergoes a β-fluoride elimination reaction to afford the target product and complete the photoredox cycle.

In conclusion, we have developed a photochemical method to generate silyl radicals from readily available silylboronic pinacol esters through homolytic substitution reactions of the boron group with amine radicals. Under mild conditions, this method excels in forming silicon-containing difluoroalkene compounds and can be scaled up to the gram level. Antifungal activity showed that at 50 μg/mL, some compounds showed >60% inhibition against *B. cinerea*, *S. turcica* and *R. solani*, with EC_{50} values comparable to or lower than commercial fungicides boscalid and pyraclostrobin. DFT and MEP analyses revealed that high-activity compounds like **8** and **13** had distinct molecular orbital distributions and electrostatic properties compared to low-activity ones. Scanning electron microscopy indicated that compound **13** effectively inhibited the mycelial growth of *B. cinerea*. These compounds serve as promising leads for developing new fungicides with optimized structures and mechanisms.

Declaration of competing interest

The authors declare that they have no known competing financial interests or personal relationships that could have appeared to influence the work reported in this paper.

CRediT authorship contribution statement

Fuyang Yue: Writing – original draft, Methodology, Investigation. **Fei Yuan:** Methodology, Investigation. **Kun Li:** Methodology, Investigation. **Xun Luo:** Methodology, Investigation. **Hongjian Song:** Writing – review & editing, Writing – original draft, Methodology, Investigation. **Yuxiu Liu:** Writing – review & editing, Writing – original draft, Methodology, Investigation. **Qingmin Wang:** Writing – review & editing, Supervision, Project administration, Funding acquisition.

Acknowledgments

We are grateful to the National Natural Science Foundation of China (No. 22271166) and the Frontiers Science Center for New Organic Matter, Nankai University (No. 63181206), for generous financial support.

Supplementary materials

Supplementary material associated with this article can be found, in the online version, at doi:10.1016/j.cclet.2025.111940.

References

[1] K.C. Mondal, S. Roy, H.W. Roesky, Chem. Soc. Rev. 45 (2016) 1080–1111.
[2] C. Chatgilialoglu, C. Ferreri, Y. Landais, V.I. Timokhin, Chem. Rev. 118 (2018) 6516–6572.
[3] S. Gately, R. West, Drug Dev. Res. 68 (2007) 156–163.
[4] B. Boury, F. Ben, R.J.P. Corriu, Angew. Chem. Int. Ed. 40 (2001) 2853–2856.
[5] T.A. Su, H. Li, R.S. Klausen, et al., Acc. Chem. Res. 50 (2017) 1088–1095.
[6] K.J. Shea, D.A. Loy, Chem. Mater. 13 (2001) 3306–3319.
[7] R.J. Hofmann, M. Vlatković, F. Wiesbrock, Polymers 9 (2017) 534.
[8] A.J. O'Lenick, K.A. O'Lenick, MRS Bull. 32 (2007) 801–806.
[9] H. Qrareya, D. Dondi, D. Ravelli, M. Fagnoni, ChemCatChem 7 (2015) 3350–3357.
[10] L. Xu, S. Zhang, P. Li, Org. Chem. Front. 2 (2015) 459–463.
[11] M. Oestreich, E. Hartmann, M. Mewald, Chem. Rev. 113 (2013) 402–441.
[12] L. Lu, J. Siu, Y. Lai, S. Lin, J. Am. Chem. Soc. 142 (2020) 21272–21278.
[13] N. Xu, B. Li, C. Wang, M. Uchiyama, Angew. Chem. Int. Ed. 59 (2020) 10639–10644.
[14] W. Guan, L. Lu, Q. Jiang, et al., Angew. Chem. Int. Ed. 62 (2023) e202303592.
[15] J. Hou, A. Ee, H. Cao, et al., Angew. Chem. Int. Ed. 57 (2018) 17220–17224.
[16] Y. Lan, X. Chang, P. Fan, et al., ACS Catal. 7 (2017) 7120–7125.
[17] X. Shang, Z. Liu, Org. Biomol. Chem. 14 (2016) 7829–7831.
[18] A. Studer, S. Amrein, Angew. Chem. Int. Ed. 39 (2000) 3080–3082.

[19] R. Zhou, Y. Goh, H. Liu, et al., Angew. Chem. Int. Ed. 56 (2017) 16621–16625.
[20] S. Chen, M. Gao, X. He, X. Shen, Nat. Commun. 16 (2025) 2468.
[21] F. Yue, J. Liu, H. Ma, et al., Org. Lett. 24 (2022) 4019–4023.
[22] W. Xu, C. Xia, Q. Shao, et al., Org. Chem. Front. 9 (2022) 4949–4954.
[23] P. Gao, L. Cui, G. Zhang, F. Chen, Catal. Sci. Technol. 13 (2023) 1628–1632.
[24] X. Yu, M. Lübbesmeyer, A. Studer, Angew. Chem. Int. Ed. 60 (2021) 675–679.
[25] R. Arai, Y. Nagashima, T. Koshikawa, K. Tanaka, J. Org. Chem. 88 (2023) 10371–10380.
[26] Z. Cai, Q. Bu, X. Wang, et al., Chem. Sci. 16 (2025) 2154–2169.
[27] J. Sang, Y. Zhang, D. Xia, et al., Org. Chem. Front. 12 (2025) 869–878.
[28] Z. Wang, N. Wierich, J. Zhang, C. Daniliuc, A. Studer, J. Am. Chem. Soc. 145 (2023) 8770–8775.
[29] F. Yue, M. Li, K. Yang, et al., Chem. Sci. 15 (2024) 14241.
[30] H. Lan, X. Huo, Y. Jia, D. Wang, Org. Lett. 26 (2024) 1011–1016.
[31] E. Speckmeier, T.C. Maier, J. Am. Chem. Soc. 144 (2022) 9997–10005.
[32] F. Yue, M. Li, F. Yuan, et al., Chin. Chem. Lett. 36 (2025) 111053.
[33] P. Jeschke, ChemBioChem 5 (2004) 570–589.
[34] Y. Pan, J. Qiu, R.B. Silverman, J. Med. Chem. 46 (2003) 5292–5293.
[35] Y. Ogawa, E. Tokunaga, O. Kobayashi, K. Hirai, N. Shibata, iScience 23 (2020) 101467.
[36] Y. Zhang, Y. Guo, Y. Zhang, S. Liu, X. Shen, Chem Catal. 5 (2025) 101200.
[37] G. Zhou, Z. Guo, S. Liu, X. Shen, J. Am. Chem. Soc. 146 (2024) 4026–4035.
[38] Y. Zhang, J. Wang, Y. Guo, S. Liu, X. Shen, Angew. Chem. Int. Ed. 63 (2024) e202315269.
[39] X. Fang, S. Wen, P. Jin, et al., ACS Catal. 12 (2022) 2150–2157.
[40] D. Deng, S. Tang, Y. Yuan, et al., Chin. Chem. Lett. 35 (2024) 109417.
[41] P. Jeschke, Pest. Manage. Sci. 66 (2010) 10–27.
[42] J. Wu, S. Zhang, H. Gao, et al., J. Am. Chem. Soc. 139 (2017) 3537–3545.
[43] F. Tian, G. Yan, J. Yu, Chem. Commun. 55 (2019) 13486–13505.
[44] F. Yue, M. Li, K. Yang, et al., Green Synth. Catal. (2025), doi:10.1016/j.gresc.2025.02.002.
[45] Y. Zhang, J. Mao, Z. Wang, L. Tang, Z. Fan, Green Chem. 26 (2024) 9371–9377.
[46] Z. Li, Y. Zhang, Y. Zhang, X. He, X. Shen, Angew. Chem. Int. Ed. 62 (2023) e202303218.
[47] F. Yue, H. Ma, P. Ding, et al., ACS Cent. Sci. 9 (2023) 2268–2276.
[48] Q. Wang, H. Song, Q. Wang, Chin. Chem. Lett. 3 (2022) 626–642.
[49] N. Wan, B.A. Woodcock, C. Scherber, et al., Science 388 (2025) 712–713.
[50] N. Zan, J. Li, J. Yao, et al., Nat. Commun. 16 (2025) 2034.
[51] C. Wei, C. Zhao, J. Li, et al., Adv. Sci. 11 (2024) 2309343.
[52] F. Che, J. Hu, M. Liao, et al., J. Am. Chem. Soc. 146 (2024) 33763–33773.
[53] Q. Tian, C. Wang, B. Liu, X. Wu, Y. Li, Adv. Sci. 12 (2025) 2502862.
[54] Q. Tian, Y. Li, Angew. Chem. Int. Ed. 62 (2023) e202302861.